Characterization and Gas Permeation Properties of Blood Compatible Membranes for Blood Oxygenators

Ana Rita Gonçalves Varandas Martins
anrivmartins@gmail.com

Instituto Superior Técnico, Lisboa, Portugal

October 2019

Abstract

Nonporous and Integral Asymmetric bi soft segment Poly(ester urethane urea) membranes were prepared including Polycaprolactone (PCL) as a second Soft Segment, using the solvent evaporation method and a modified version of phase inversion technique, respectively. The synthesis was performed by reacting a combination of Polyurethane (PUR) and Polycaprolactone-diol prepolymers in a solvent mixture comprising Dimethylformamide (DMF) and Diethyl ether (DEE).

Several casting solutions were made with a total polymer/solvent weight ratio of 65/35, a DMF/DEE ratio of 3/1 wt.% and varying the PUR/PCL weight ratio (100/0, 95/5, 90/10 and 85/15). For asymmetric membranes, solvent evaporation times of 1, 5 and 10 minutes were studied. Samples were analysed by Scanning Electron Microscopy (SEM).

Using an existing gas permeation setup it was possible to determine the permeances for the two groups of membranes. Plus, applying the time lag method to the same results allowed the determination of the diffusion and solubility coefficients. All results showed the same order of magnitude.

No immediate correlation was identified between the properties studied due to its nonlinear behavior, however, from the overall comparison, the best compositions and, consequently, preparation methods were revealed to be 5% PCL with 5 minutes of solvent evaporation time and 15% PCL with 1 minute. Estimates made on the thickness of the dense layer revealed that the synthesis of asymmetrical membranes allowed a reduction of this variable, in contrast to fully dense membranes, representing an improvement in gas permeation.

Keywords: Membrane blood oxygenators, Bi soft segment Poly(ester urethane urea) membranes, Integral asymmetric membranes, Gas permeation, Time lag method.

1. Introduction

ECMO, also known as Extracorporeal Membrane Oxygenation, is a procedure used to oxygenate blood, as well as removing carbon dioxide from it, without the need for native lungs. On that note, this equipment takes over the work of the lungs, heart or both when these organs are too damaged to perform their function properly, allowing the healing process to occur, or during surgery [1]. This extracorporeal life support consists in an external artificial circulation that carries venous blood, lacking in O_2 content but rich in CO_2, from the patient to a gas exchange device where blood then becomes enriched with the first mentioned above and has carbon dioxide removed. The exchange is achieved by feeding the said gases and a sweep gas to a compartment divided by a membrane. This device is called an oxygenator and the blood is then warmed and returned to the body [2].

The ideal oxygenator must be capable of performing an efficient gas exchange and, at the same time, should be gentle to the blood. On that note, the equipment must deliver about 250 cm^3 (STP)/min O_2 and remove about 200 cm^3 (STP)/min CO_2. It is important to refer that the driving force for O_2 transfer is 15 times than the one for CO_2. Moreover, in the lung, the ratio is about 13 times, but this organ is over 20 times more permeable to the second than to the first mentioned gas. Therefore, the key consideration in the design of a membrane oxygenator is the CO_2 transport [3].

In the history of oxygenators, three different types are known: film, bubble and membrane. The first one consists in producing a thin blood film where the gas exchange takes place on the surface of the exposed blood film. Secondly, bubble type oxygenators work by introducing gas directly into the blood in the form of bubbles. In this type of equipment, gas exchange is enhanced due to the large surface area of the bubbles which makes it one of the most effective, but introducing air bubbles directly into the blood causes mechanical stress on the system. Lastly, there are several types of membrane oxygenators, for example: plate-type membrane, disposable coiled membrane and hollow-fibre. The advantages rely on requiring smaller volumes for priming to achieve a sufficient gas transfer rate and also contributing for less blood trauma such as hemolysis, because it uses a similar mechanism to the natural lung [1, 4].

Previous studies have addressed the synthesis of bi soft segment polyurethane urea membranes, characterized by the presence of two different types of Soft Segments: poly(propylene oxide) (PPO) and poly(caprolactone) (PCL) and prepared by extending a poly(propylene oxide) based tri-isocyanated prepolymer with poly(caprolactone) diol [5]. Said studies also showed that the variation of the ratio of PU to PCL diol content in the membrane formulation altered the surface energy, phase morphology both in the bulk and near the surface and affected hemocompatibility. Plus, the increase of PCL diol content lead to smoother blood-contacting surfaces, more hydrophilic and with higher maximum zeta potentials. Regarding hemocompatibility, all different compositions resulted in nonhemolytic membranes for a contact time with blood of 3 hours [5, 6].

Furthermore, gas permeation tests on nonporous membranes concluded that 10% PCL content ones exhibited the highest CO_2 permeation followed by the 5% and 0%, opposing to the 15% that presented the lowest CO_2 permeation values. Plus, the permeability coefficients varied with PCL content and the results were 188, 250, 337 and 113 Barrer for 0%, 5%, 10% and 15%, respectively. For O_2, permeability coefficients don't vary significantly, remaining approximately constant for all the membranes. Diffusion coefficients for CO_2 increased in order of 5, 15, 0 and 10% [7]. For integral asymmetric bi soft segment poly(ester urethane urea) membranes synthesized by a novel procedure, based on a modification of phase inversion technique, experimental tests exhibited CO_2 permeances in the range required for membrane oxygenators, opposing to the O_2 permeances still needing improvements [8].

2. Experimental

2.1. Materials and Methods

2.1.1 Synthesis of Poly(ester urethane urea) Membranes

For the preparation of bi soft segment poly(ester urethane urea) membranes two prepolymers were used: Poly(propylene oxide) (PPO) based Polyurethane with three isocyanate terminal groups, from Fabrires-Produtos Químicos, SA, and Poly(caprolactone) diol with a molecular weight of approxi-

mately 530 Da, from Sigma-Aldrich, being the chain extending prepolymer.

Regarding the solvents, the synthesis was performed using Dimethylformamide (DMF) (w/w%grade, 99.8%) and Diethyl ether (DEE) (w/w% grade, 99.5%) both supplied by Panreac. As a catalyst Tin(II)-ethylhexanoate (wt.% 95%) from Sigma-Aldrich was used.

Nonporous and Integral Asymmetric bi soft segment Poly(ester urethane urea) membranes were prepared adopting the solvent evaporation method and a modified version of phase inversion technique, respectively. It is important to refer that DMF/DEE and polymer/solvents ratios were kept constant and equal to 3:1 and 65/35 wt.%, respectively, throughout the study. For asymmetric membranes solvent evaporation times of 1, 5 and 10 minutes were applied. The casting was performed using a 250μm casting knife.

The nomenclature adopted is detailed in the table below.

Table 1: Designations, chemical compositions and solvent evaporation times of PU membranes synthesized by varying PCL content.

Membrane	PUR/PCL (wt.%)	Solvent Evaporation Time (min)
PU0	100/0	-
PU5	95/5	-
PU10	90/10	-
PU15	85/15	-
PU5-1	95/5	1
PU10-1	90/10	1
PU15-1	85/15	1
PU5-5	95/5	5
PU10-5	90/10	5
PU15-5	85/15	5
PU5-10	95/5	10
PU10-10	90/10	10
PU15-10	85/15	10

2.1.2 Gases

Gas permeation tests were performed using gases provided by Air Liquid, more specifically, oxygen (purity $\geq$ 99.5%), carbon dioxide (purity $\geq$ 99.98%) and nitrogen (purity $\geq$ 99.999%).

2.2. Scanning Electron Microscopy (SEM)

All the synthesized membranes were observed by Scanning Electron Microscopy (SEM) using a Hitachi S-2400 SEM microscope (Hitachi, Tokyo, Japan). For the observation, multiple samples were prepared by fracturing parts of the specific membrane after being freezed with liquid nitrogen. These small pieces were then mounted on a stub and sputter-coated with gold. Images of the top, cross sections and bottom surfaces for each sample were taken.

2.3. Gas Permeation Setup and Tests

Gas permeation tests were performed in a setup built by Eusebio, T. [9]. Later, the same setup was optimized by Pon, P. [10] allowing the elimination of problems such as low reproducibility and high uncertainty associated for more permeable membranes. The transient state was then possible to observe in measurements with O_2 and N_2, enabling the determination of the diffusion and solubility coefficients for these gases by the time lag method.

The setup was designed including a vacuum pump to make sure the system was gas free before any measurement, obeying the initial and boundary conditions applied in the Fick's Second Law of diffusion, since the goal was to obtain more precise gas permeation measurements of membranes.

Furthermore, the apparatus consists of a permeation cell, a Feed Pressure Sensor (PfT) (Setra, Model 205, Massachusetts, USA), a Permeate Pressure Transmitter (PpT) (Intelligent Transmitter Paroscientific, Series 6000, model 6100A-CE Inc. Washington, USA) attached to a Paroscientific model 710 display unit, which is connected to a computer, a small cylinder with a volume of 12.6$\pm$0.1 cm^3 (Cylinder 1) and a big cylinder with a volume of 167.2$\pm$0.2 cm^3 (Cylinder 2). Lastly, the tubing system in the receiving chamber has a volume of 13.5$\pm$0.01 cm^3, composed by tubes of stainless steel 316 with an external diameter of 1/8 inch (Hoke®), needle valves (3700 Series, Hoke®) and tube fittings made of stainless steel, titanium and brass (Gyrolok®). The total volume of the permeate side is 193.3$\pm$0.3 cm^3. A schematic diagram of this installation is depicted in figure 1.

The equipment was installed in a thermostatic system (air bath) which consists of a wine fridge (cold source), a resistance thermometer, a heater connected to a PID controller and a fan to homogenize the inner temperature. The variation of the pressure was recorded with the software Digiquartz ® version 2.0 (Paroscientific Inc, Washington, USA).

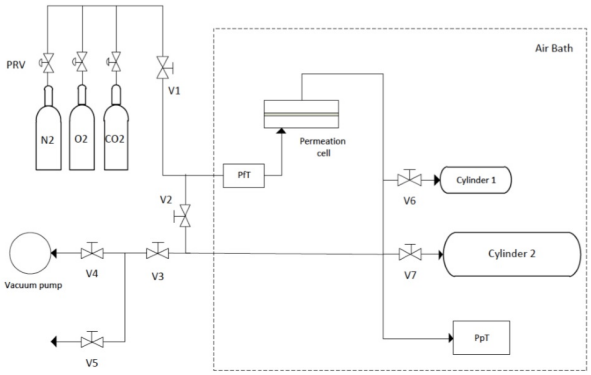

Figure 1: Schematic representation of the gas permeation Setup [10].

Concerning the permeation cell itself, the membrane is placed between two plates of stainless steel with an active surface area of 9.62 cm^2.

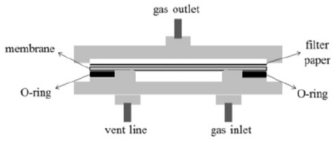

Figure 2: Schematic representation of the permeation cell.

To initiate the measurements, the setup must be thermostated to a temperature of approximately 37ºC$\pm$0.2ºC. After, valves V2 and V3 must be closed, maintaining the vacuum provided by the pump. Secondly, the pressure of the gas being fed (O_2, CO_2 or N_2) has to be regulated on the pressure reducing valve (PRV) in the gas cylinder, while valve V1 is closed. Finally, valve V1 can be opened and permeation begins to be recorded as a function of time by the PpT sensor.

Once the membrane is inserted in the cell, it is possible to determine the gas flux through it by monitoring the variation of pressure with time. During the experiment, the value given by the PfT must be checked to make sure it's value is constant throughout the test.

In the end, the reverse process is adopted by closing valve V1 and opening valves V2 and V3, ensuring that the setup is completely degassed before the next measurement. It is important to mention that valve V5 is always closed, except when there is the need to return to atmospheric pressure, and valves V6 and V7 are opened or closed depending on the gas that is being measured due to the sensitivity of the system. Thus, permeation measurements of oxygen and nitrogen were carried out with both valves V6 and V7 closed, which corresponds to a volume of 13.5 cm^3, while for carbon dioxide both valves were opened making up a volume of 193.3 cm^3.

3. Results and Discussion

3.1. Surface and Cross-section characterization by SEM

3.1.1 Nonporous Poly(ester urethane urea) membranes

Samples of the nonporous membranes prepared with 0, 5, 10 and 15 wt.% PCL, DMF/DEE and polymer/solvent ratios of 3:1 and 65/35 wt.% were observed by Scanning Electron Microscopy. Images similar to the ones reported in figure 3 were obtained to all four membranes studied.

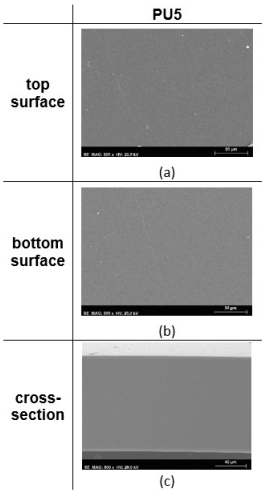

Figure 3: Images of the top/bottom surfaces and cross-sections obtained by SEM: (a) top surface, (b) bottom surface and (c) cross-section of membrane PU5.

It was possible to confirm that all the compositions studied result in totally dense membranes once there is no sign of any visible pores. All the cross-section images obtained for the PU0, PU5, PU10 and PU15 show the symmetrical character of these membranes. When ready to use, said membranes are transparent, very sticky and slightly elastic.

Average total membrane thickness was determined from 4 different measurements in each sample using a digital caliper. Table below presents these values as well as the respective standard deviations.

Table 2: Average thicknesses and respective standard deviations for nonporous membranes PU0, PU5, PU10 and PU15.

Membrane	Thickness, δ (mm)
PU0	0.112±0.006
PU5	0.115±0.004
PU10	0.107±0.004
PU15	0.112±0.001

Observing the results of the measurements performed manually and comparing with the images obtained through SEM, it is possible to notice a greater membrane thickness for an intermediate composition of 5% PCL, in both cases. In addition, the SEM analysis performed in all the PU membranes revelead a slight decrease in thickness from the membrane without the second prepolymer to the two membranes with larger quantities, a qualitative observation that was not reflected in the measurements made with the digital caliper.

3.1.2 Integral Asymmetric Poly(ester urethane urea) membranes

Following the same procedure adopted in section 3.1.1, diverse samples of the synthesized membranes, varying the PCL content and solvent evaporation time, were observed by Scanning Electron Microscopy to study the influence of said parameters in membrane morphology. In figure 4 is represented the images gathered for membrane PU15-1.

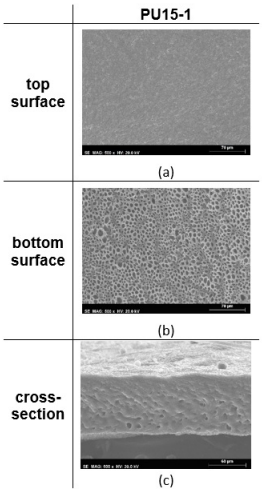

Figure 4: Images of the top/bottom surfaces and cross-sections obtained by SEM: (a) top surface, (b) bottom surface and (c) cross-section of membrane PU15-1.

Analyzing the images gathered for 1 minute of solvent evaporation time, it was observed that the amount of pores present on the top surface decreases with the increase in PCL concentration. On the other hand, on the bottom surface, the exact opposite occurred since with the increase in PCL content there was an increase in pore density, with the consequent appearance of pores with a larger diameter. Finally, it is important to mention that the visual analysis performed on all the SEM images of all the integral asymmetric membranes' cross sections revealed a decrease in their thicknesses with their larger contents of prepolymer. Such observation reinforced the accuracy of the manually measured thicknesses presented in the table 3.

Additionally, images referring to the second solvent evaporation time studied - 5 minutes - enabled the conclusion that in the present case, an increase in the amount of PCL did not reflect major changes in the characteristics of the top surface of the membranes, only a minor extinction of the residual pores existing in the first composition. In contrast, on the bottom surface the pore density increases with the concentration of PCL as well as the size of the pores. Lastly, from the observation of the cross sections it was possible to verify that in the core of the membrane, for a concentration of Poly(caprolactone) equal to 10%, the porosity is higher than in the other compositions.

Compared to what was previously stated above, SEM images obtained for the last solvent evaporation time of 10 minutes revealed that the top surface of the membrane suffered a slight increase in porosity with the increase in PCL content. As for the bottom surface, again an increase in polymer concentration reflected an increase in porosity as well as individual pore size. Also, the observation of the cross sections made it possible to verify that for a PCL amount equal to 10% the membrane's core showed a higher porosity and larger pores than the other compositions. The decrease in membrane thickness was also visible with the increase of PCL.

Comparing the three different times, and thus also perceiving the effect of the increase of the solvent evaporation time on the morphology of the membranes, a decrease of the pore density on the top surfaces is visible with the increase in time, except for the membranes with composition equal to 15% PCL. Moreover, the size of the pores does not seem to have any direct relation with the increase of solvent evaporation time.

In general, a lower/nonexistent porosity in the top surface in relation to the bottom surface was noticeable, exhibiting what appears to be a dense thin superficial layer. These dense layers were most visible in all membranes containing 15% PCL. When ready for testing, porous membranes had a whitish and opaque appearance, were more elastic and easier to operate than nonporous.

Similarly, average total membrane thickness was determined from 4 different measurements and are displayed in table 3.

Table 3: Average thicknesses and respective standard deviations for integral asymmetric membranes.

Membrane	Thickness, δ (mm)
PU5-1	0.118±0.004
PU10-1	0.117±0.004
PU15-1	0.102±0.002
PU5-5	0.107±0.004
PU10-5	0.109±0.004
PU15-5	0.103±0.005
PU5-10	0.121±0.002
PU10-10	0.121±0.002
PU15-10	0.110±0.003

Its noticeable that membranes with higher contents in PCL were somewhat thinner than the 5 and 10 wt.%. Besides that, the values obtained were in accordance between different samples.

On a further note, obtaining different surface and internal morphological characteristics may require an optimisation process of the membrane preparation method, such as the variation of the solvent and/or polymer/solvent ratio.

3.2. Gas Permeation Experiments

3.2.1 Nonporous Poly(ester urethane urea) membranes

To evaluate gas permeation of the membranes synthesized and observed by SEM, several experiments were run applying a constant volume method where the pressure evolution was recorded, using the apparatus described in section 2.3. The tests were performed with multiple feed pressures.

Each experiment gives back a permeation curve which consists on the pressure evolution on the permeate side as a function of time. Similar curves were obtained for all 4 membranes at different feed pressures.

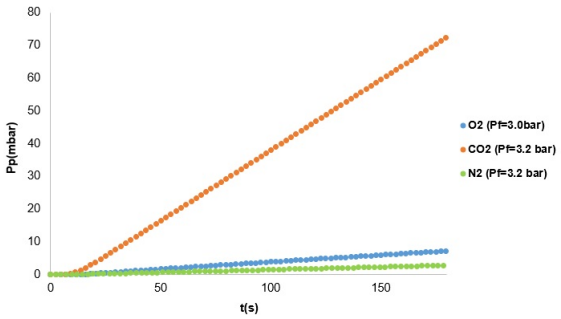

Figure 5: Permeation curves of gases O_2, CO_2 and N_2 for PU5 membrane.

From figure 5 is possible to acknowledge the presence of two distinct zones in every curve: the first and constant corresponding to the transient state and the second, where a progressive increase of pressure is registered, the steady state. Also, a clear conclusion to take is that, for similar feed pressures, the slope of the steady state increases in order of N_2, O_2 and CO_2, as seen before by Pon [10].

Moreover, the slope, dp_p/dt, of every steady state zone enabled the calculation of one volumetric flux, J, by converting this value to a volumetric flow and dividing it by the effective membrane area, A.

Representing the plots of this variable as a function of the transmembrane pressure (TMP), defined as the difference between the feed pressure, p_f, and the initial permeate pressure, p_{pi} (TMP=(p_f-p_{pi})), allowed the tracing of the figures 6, 7 and 8. In the present cases, since the system was placed under vacuum before the beginning of every test, the value of the later variable is equal to 0.

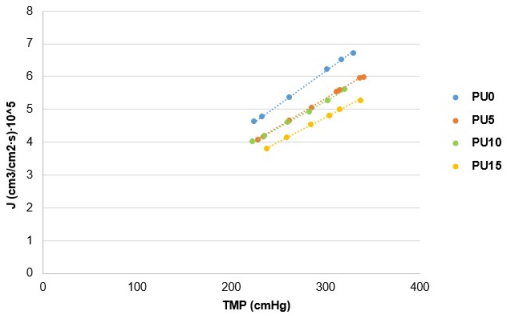

Figure 6: Volumetric fluxes as a function of TMP for O_2.

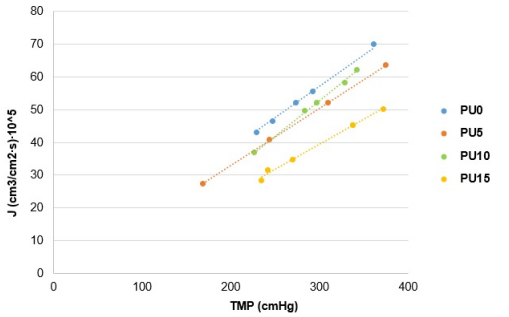

Figure 7: Volumetric fluxes as a function of TMP for CO_2.

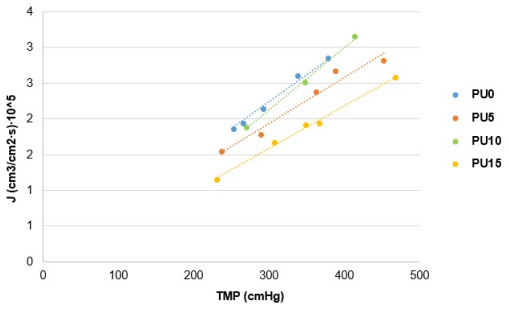

Figure 8: Volumetric fluxes as a function of TMP for N_2.

Putting together the previous conclusions collected and observing the results, would be expected not only an increase of the fluxes of permeation in order of N_2, O_2 and CO_2, but also a linear relationship between the two variables involved tending to the point (0,0), meaning that for a transmembrane pressure of 0 cmHg the flow through the membrane is equal to 0 cm^3/cm^2s, which was confirmed. It is also important to note that the highest fluxes were obtained for PU0 while the lowest were observed for PU15.

Having now in mind the behavior of the fluxes as a function of TMP for all 4 membranes studied, from the slopes of the said plots, it was possible to obtain the permeances, $perm$. Furthermore, due to the fact that this values greatly depend on the thickness of the membranes and since it varied from sample to sample, the permeances were converted to permeability coefficients applying expression 1 - table 4 and figure 9.

$$P = perm \times \delta \times 10^{10} \quad (1)$$

where P is the permeability coefficient in Barrer units.

The standard deviation values presented in the table were determined based on the calculation of two different permeability values from two distinct gas permeation tests, each one with a respective deviation. Thus, it corresponds to a rough estimate of the error.

Table 4: Average permeability coefficients obtained for N_2, O_2 and CO_2, using nonporous membranes PU0, PU5, PU10 and PU15.

	P (Barrer)		
Membrane	N_2	O_2	CO_2
PU0	9.9	22.9±0.4	230±0
PU5	7.4	20.1±0.3	198.3±1.3
PU10	10.1	18.2±0.4	218.0±36.1
PU15	6.7	16.5±0.5	168.1±0.5

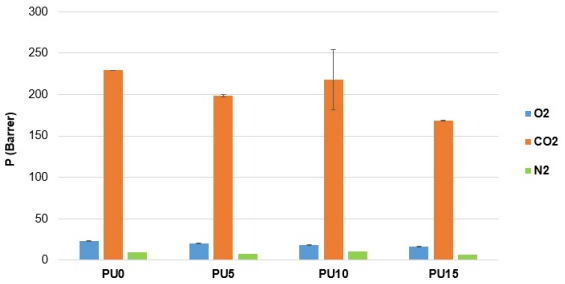

Figure 9: Average permeability coefficients obtained for N_2, O_2 and CO_2, using nonporous membranes PU0, PU5, PU10 and PU15.

Regarding the results obtained in the experiments, by analyzing the table and respective figure above, it is clear that the permeability coefficients for the oxygen are decreasing with the increase in PCL content. However, N_2 and CO_2 values did not obey the previous tendency. Overall, membrane PU0 showed the highest values of permeability, except for nitrogen.

Studies carried by Faria et. al [7], revealed that the CO_2 permeability coefficients varied with PCL content and was 188 Barrer for 0%, 250 Barrer for 5%, 337 Barrer for 10% and, finally, 113 Barrer for 15%. This tendency is observed also in the results shown in table 4 above, except for the membrane with less wt.% in PCL. On the other hand, values from the present work are slightly lower for membranes with 5% and 10% PCL opposing to the 0% and 15% ones being higher than expected. Additionally, was estimated that P_{CO_2} values were 10-30 times higher than P_{O_2} which was also verified.

Previous results gathered by Pon, G. [10], showed lower P_{CO_2} and higher P_{O_2} values to the 10% PCL membrane (208 Barrer and 21 Barrer, respectively), as well. It is important to note that these values were determined using the same PCL prepolymer and the same membrane preparation technique, contrary to the study carried out by Faria et. al. It is also important to mention that the thicknesses used in the latter were significantly higher.

Comparing with other existing membranes used for artificial lungs, for example, Polypropylene (PP) and Polymethylpentene (PMP), permeability coefficients present values of 2-2.2 Barrer and 30-32.3 Barrer for P_{O_2} and 9-9.2 Barrer and 90-92.6 Barrer for P_{CO_2}, respectively. On that note, it can be affirmed that nonporous Poly(ester urethane urea) represent an improvement in gas permeability for both gases [11, 12]. However, it is important to keep in mind that the studies carried out in this work were performed in a gas/membrane/gas setup and not in a gas/membrane/liquid system. Thus, the resistance imposed to gas transport is higher and for that reason it is plausible to admit that the permeance values obtained in this work could be equivalent to those stated for existing artificial lungs.

In order to complete the study of permeabilities, ideal selectivities were also computed applying equation 2. Results are presented in table 5.

$$\alpha_{A/B} = \frac{\mathrm{Perm_A}}{\mathrm{Perm_B}} = \frac{\mathrm{P_A}}{\mathrm{P_B}} \tag{2}$$

Table 5: Ideal selectivities and respective standard deviations for nonporous Poly(ester urethane urea) membranes.

	α		
Membrane	**O_2/N_2**	**CO_2/N_2**	**CO_2/O_2**
PU0	2.31±0.04	23.13±0.0	10.02±0.18
PU5	2.71±0.05	26.77±0.17	9.89±0.18
PU10	1.80±0.04	21.54±3.57	11.99±2.00
PU15	2.46±0.07	25.01±0.07	10.17±0.31

Previous studies showed that higher permeabilities correspond to lower selectivities [13], which is confirmed by the results in both tables 4 and 5.

Finally, an ANOVA test was executed to permeability results reported above. In particular, this test determines what is the probability that all data groups are the same, i.e, if the differences between different groups are due the users' actions, differences within groups are what was expect of differences between data or are simply caused by the noise or variability. Therefore, was proved that, for a confidence level of 95%, there is a significant difference between the mean values.

3.2.2 Determination of the Total Surface Area required

As specified in section 1 the ideal oxygenator must deliver about 250 cm^3 (STP)/min O_2 and remove about 200 cm^3 (STP)/min CO_2 [3].

The surface areas were then estimated to meet said specifications for all four membranes by extrapolating the flux value for a pressure of 2.0 bar, based on the graphs illustrated in figure 6 (table 6).

Table 6: Membrane surface areas estimated to meet specifications of oxygenators and respective volumetric fluxes.

	J × 10^{-5} (cm^3/cm^2s)		**Surface Area (m^2)**	
Membrane	O_2	CO_2	O_2	CO_2
PU0	3.1	28.6	13.5	1.2
PU5	2.7	25.3	15.7	1.3
PU10	2.6	26.4	15.8	1.3
PU15	2.4	19.7	17.5	1.7

As expected, higher fluxes of gas passing through the membrane are associated to lower transfer areas.

The improvements verified on permeability coefficients for carbon dioxide turned into smaller surface areas required to execute the correct gas exchange. On the other hand, for oxygen, it would require a total membrane surface area of approximately 13 to 17 m^2 which is an order of magnitude higher than the average membrane surface area of commercial oxygenators.

3.2.3 Determination of Diffusion and Solubility Coefficients

Gas permeation experiments also allowed the determination of diffusion and solubility coefficients through further analysis of the permeation curves. Calculations were based on the time lag method (equation 3) [14]. The practical application of this method consists on tracing the steady state asymptote and determine its interception with the x axis (time axis), as exemplified in figure 10.

$$\mathrm{t_{lag}} = \frac{\delta^2}{6\,\mathrm{D_i}} \tag{3}$$

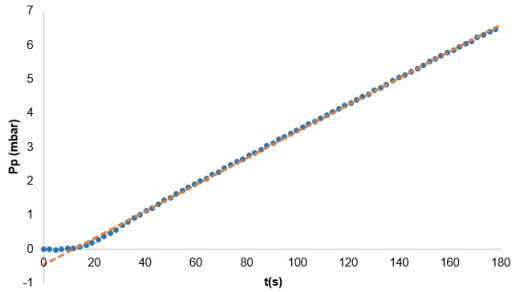

Figure 10: Example of the procedure adopted when determining the time lag, performed on a O_2 permeation curve for PU10 membrane.

Later on, knowing the several time lag values, diffusion coefficients were obtained (table 7 and figure 11).

Table 7: Average diffusion coefficients and respective standard deviations for nonporous membranes: PU0, PU5, PU10 and PU15.

	$D \times 10^{-6}$ (cm^2/s)		
Membrane	N_2	O_2	CO_2
PU0	1.40±0.05	2.14±0.44	1.66±0.15
PU5	1.22±0.11	1.91±0.16	1.63±0.15
PU10	1.22±0.14	1.59±0.20	1.36±0.08
PU15	1.00±0.02	1.74±0.12	1.42±0.08

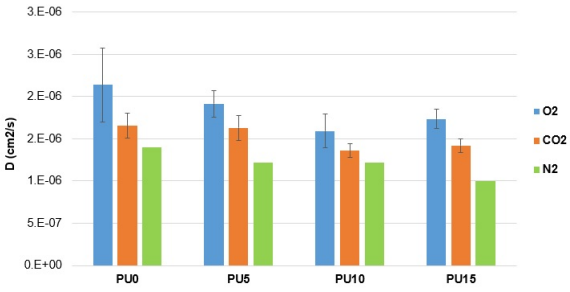

Figure 11: Average diffusion coefficients and respective standard deviations for nonporous membranes: PU0, PU5, PU10 and PU15

Analysing the results given on table 6.6, it appears to reveal a tendency which is a decrease of diffusion coefficients from PU0 to PU10, for the three gases. For membrane PU15, although this variable increases again, it is always lower than the values obtained for PU0 and PU5, except for N_2 where D assume the lowest result registered.

Additionally, it would be expected that diffusion coefficients increase in order of N_2, O_2 and CO_2 once the size of the gas molecules decreases in that order (3.64 Å, 3.46 Åand 3.30 Å, respectively) [13, 15]. However, instead of the tendency mentioned above, variable D increased in order of N_2, CO_2 and O_2. A possible explanation is the fact that carbon dioxide is considered to be an interacting gas, while oxygen and nitrogen are non-interacting gases, increasing resistance to diffusion [16].

Starting from the values reported in table 7, solubility coefficients were easily obtained applying expression 4, since in nonporous membranes the main mechanism of transport is commonly explained by the solution diffusion mechanism. Table 8 resumes the average solubility coefficients and respective standard deviations for nonporous Poly(ester urethane urea) membranes.

$$\mathrm{P} = \mathrm{S}\,\mathrm{D} \tag{4}$$

Table 8: Average solubility coefficients and respective standard deviations for nonporous membranes: PU0, PU5, PU10 and PU15.

	$S \times 10^{-4}$ (cm^3/cm^3cmHg)		
Membrane	N_2	O_2	CO_2
PU0	7.07±0.24	11.13±1.68	140.01±11.80
PU5	6.14±0.60	10.64±0.93	123.25±12.92
PU10	8.40±1.00	11.86±2.14	160.03±8.50
PU15	6.74±0.16	9.62±1.21	119.22±7.38

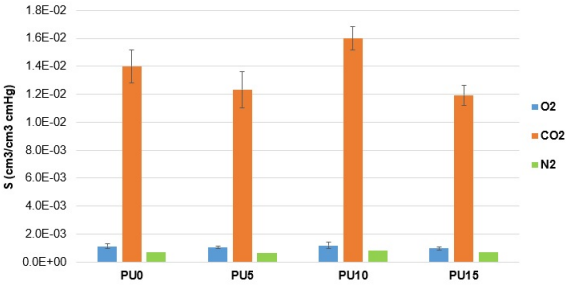

Figure 12: Average solubility coefficients and respective standard deviations for nonporous membranes: PU0, PU5, PU10 and PU15

Solubility is greatly controlled by the ease of condensation of the gas molecules [16]. On that note, keeping in mind that the boiling points increase in order of N_2, O_2 and CO_2 [15], the latter is the most likely to condensate. Moreover, it is noteworthy to mention that the work temperature used during the gas permeation tests (37ºC) is very close to the critical point of carbon dioxide, which is 31.1ºC. The remaining two gases present critical temperatures below 0ºC, meaning that even if the temperature is maintained and the pressure is greatly increased, the condensation of both gases will be impossible to achieve [15]. Results obtained on the presented experiments verify this fact since higher solubilities were registered for carbon dioxide, followed by oxygen and, finally, nitrogen.

As observed before for permeability results for N_2 and CO_2, experiments did not reveal a tendency between solubility coefficient values as the PCL content was varied. More specifically, PU10 showed always higher values when compared to other wt.%, followed by PU0, while PU15 exhibited the lowest permeability coefficients, except for N_2.

Comparing the results obtained in the present work with the values from previous studies [7], it was possible to note that for both variables D and S no tendency was evidenced on the study also. Furthermore, every value determined on this work is higher than the ones found on the study.

Overall, since it is a process controlled by solubility, that is, an increase in solubility will have a greater impact than an increase in the diffusion coefficient, the low permeability registered for N_2 when compared to O_2 and CO_2 can be explained and supported by the low solubility, reflected in low diffusion. Moreover, higher permeabilities mostly result in higher solubility coefficients. Lastly, 0% PCL membrane showed always higher permeabilities and diffusion coefficients while PU10 revealed higher solubility coefficients.

Similarly to permeabilities, it is important to note that ANOVA tests were run to all the results presented above and was proved that, for a confidence level of 95%, there was a significant difference between the mean values for diffusion coefficients, as well as for solubility coefficients.

3.2.4 Integral Asymmetric Poly(ester urethane urea) membranes - Different solvent evaporation times

As previously performed on nonporous Poly(ester urethane urea), to evaluate gas permeation of integral asymmetric membranes, several experiments were run applying a constant volume method where the pressure evolution was recorded, using the apparatus described in section 2.3. The tests were performed with multiple feed pressures, as well.

Plots with fluxes as a function of transmembrane pressure were drawn. These plots are organised by membrane type (wt.% PCL and solvent evaporation time) and permeated gas.

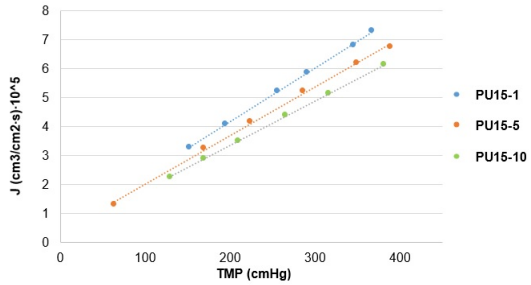

Figure 13: Volumetric fluxes as a function of TMP for integral asymmetric PU15 with solvent evaporation times of 1, 5 and 10 minutes for O_2.

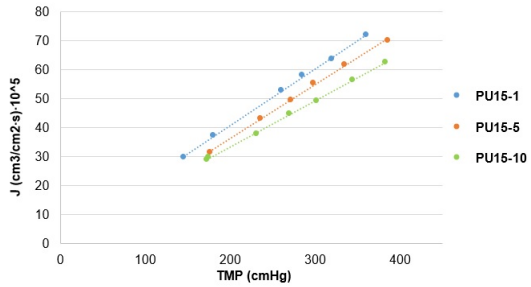

Figure 14: Volumetric fluxes as a function of TMP for integral asymmetric PU15 with solvent evaporation times of 1, 5 and 10 minutes for CO_2.

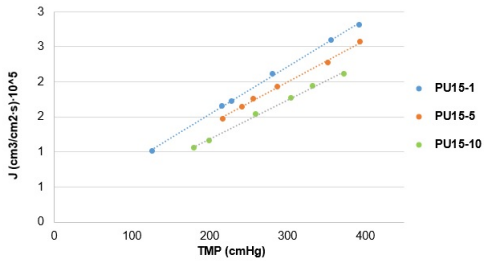

Figure 15: Volumetric fluxes as a function of TMP for integral asymmetric PU15 with solvent evaporation times of 1, 5 and 10 minutes for N_2.

As observed for nonporous membranes, the highest fluxes were registered for CO_2, followed by O_2 and then N_2, as then checked by analyzing all nine membranes through plots identical to the ones reported above (figures 13, 14 and 15).

From the plots corresponding to 5% and 10% PCL, a clear conclusion to take was the inversion of order for membranes with 1 minute and 5 minutes of solvent evaporation. Keeping in mind the procedure used to prepare integral asymmetric membranes, in principal, longer evaporation times would correspond to thicker dense layers and, consequently, less permeation fluxes. However, this tendency is only revealed for 15 wt.% PCL (figures 13, 14 and 15). Again, irregularities in the thickness of the whole membrane taken from the glass and from which the samples were taken can cause differences in the thickness of each sample itself, increasing the disparity of the results.

Once more, as a result of the treatment of the slopes it was possible to determinate the permeances, $perm$, for each case. Results are synthesized in table 9.

In this regard, although some differences were visible between compositions and solvent evaporation times since the fluxes measured were distinct, it was noticeable that the slopes, more specifically the permeances, did not vary so significantly and were the same order of magnitude.

Membranes synthesized with 5% and 10% PCL and a solvent evaporation time of 5 minutes showed the highest permeances, followed by those with 1 minute and 10 minutes, while 15 wt.% PCL membranes exhibited decreasing values in order of 1, 5 and 10 minutes.

Table 9: Average permeances determined for integral asymmetric membranes: PU5-1, PU5-5, PU5-10, PU10-1, PU10-5, PU10-10, PU15-1, PU15-5 and PU15-10, prepared with different solvent evaporation times.

	Perm ($cm^3/cm^2\,s\,cmHg)\times10^{-5}$		
Membrane	**O_2**	**CO_2**	**N_2**
PU5-1	0.0180	0.190	0.0066
PU5-5	0.0188	0.200	0.0070
PU5-10	0.0160	0.165	0.0062
PU10-1	0.0162	0.165	0.0060
PU10-5	0.0169	0.179	0.0067
PU10-10	0.0145	0.154	0.0053
PU15-1	0.0187	0.200	0.0068
PU15-5	0.0175	0.184	0.0060
PU15-10	0.0155	0.161	0.0055

3.2.5 Integral Asymmetric Poly(ester urethane urea) membranes - Different PCL contents

The set of data gathered during the experiments made it possible to evaluate if there was any type of correlation between the amount of PCL polymer in the membranes and the permeability properties, as well.

Figures 16, 17 and 18 equally represent plots of the volumetric fluxes as a function of transmembrane pressure (TMP) for every composition studied (5%, 10% and 15% PCL), maintaining the solvent evaporation time constant of 1 minute. Note that similar plots were drawn to the remaining solvent evaporation times (5 and 10 minutes).

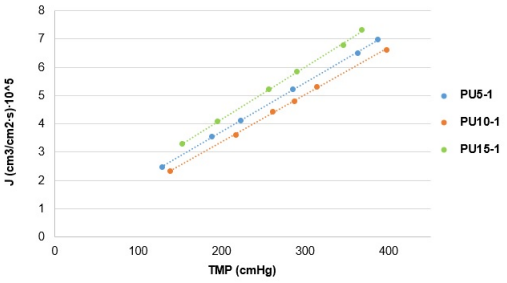

Figure 16: Volumetric fluxes as a function of TMP for integral asymmetric PU5, PU10 and PU15 with solvent evaporation time of 1 minute for O_2 permeation.

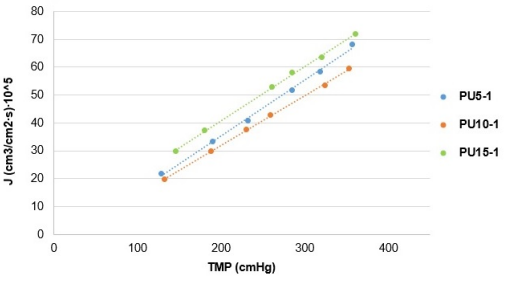

Figure 17: Volumetric fluxes as a function of TMP for integral asymmetric PU5, PU10 and PU15 with solvent evaporation time of 1 minute for CO_2 permeation.

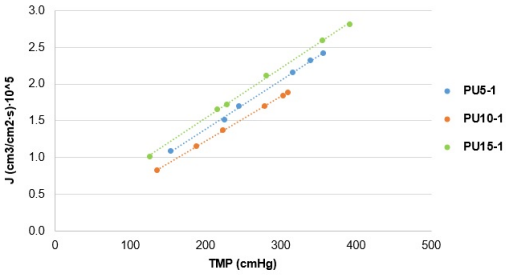

Figure 18: Volumetric fluxes as a function of TMP for integral asymmetric PU5, PU10 and PU15 with solvent evaporation time of 1 minute for N_2 permeation.

Analyzing all the graphs, the good performance of the membranes synthesized with the lowest and highest amount of PCL was evidenced. On the reverse, in general, the intermediate composition registered the lowest volumetric fluxes. It is also important to point out the membrane inversion for evaporation times of 1 and 5 minutes, in other words, while for the first evaporation time the membrane that revealed the highest flux was the one with the highest amount of the mentioned polymer (15 wt.%), for the second was the one with the lowest composition (5 wt.%) that was the one exceeding the remaining ones. Finally, for 10 minutes of solvent evaporation time the results are quite balanced between membranes.

Observing all results synthesized in table 9, the lower values were always obtained for 10% PCL membrane, excepting for N_2 with 5 minutes of solvent evaporation. Respecting the other two compositions, when prepared with 5 and 10 minutes a decrease in permeance was verified from the 5 to 15% PCL for O_2, CO_2 and N_2. For membranes with 1 minute of solvent evaporation, the opposite was observed instead. With this being said, it was not possible to find a direct correlation between the amount of PCL and the permeances with the same trend observed for the fluxes being followed as seen before in section 3.2.4.

3.2.6 Comparing Nonporous with Integral Asymmetric Poly(ester urethane urea) membranes

With the goal of comparing the gas permeation characteristics of both nonporous and integral asymmetric Poly(ester urethane urea) (PEUU) membranes and investigate if there was any benefits on using the latter on actual blood oxygenators, once it was not possible to compare permeabilities or diffusion and solubility coefficients, the volumetric fluxes obtained during the experiments were gathered in the same figures.

To illustrate the kind of graphs analysed, below are represented the plots drawn for 15% PCL membranes with 1, 5 and 10 minutes solvent evaporation times, as well as the dense membrane, that resulted from the permeation of oxygen, carbon dioxide and nitrogen.

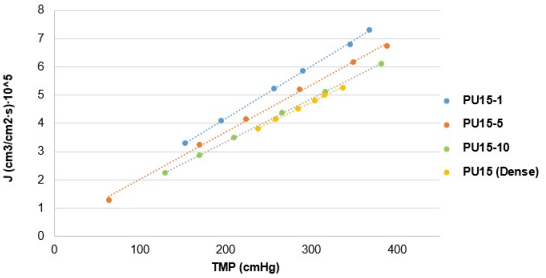

Figure 19: Volumetric fluxes as a function of TMP for dense PU15 and integral asymmetric PU15 with solvent evaporation times of 1, 5 and 10 minutes, for O_2 permeation.

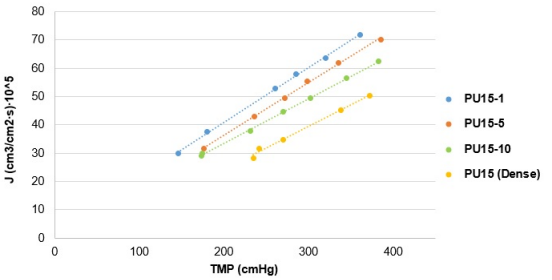

Figure 20: Volumetric fluxes as a function of TMP for dense PU15 and integral asymmetric PU15 with solvent evaporation times of 1, 5 and 10 minutes, for CO_2 permeation.

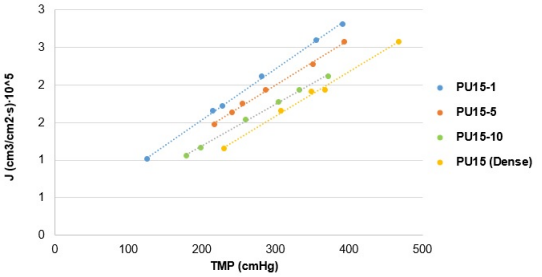

Figure 21: Volumetric fluxes as a function of TMP for dense PU15 and integral asymmetric PU15 with solvent evaporation times of 1, 5 and 10 minutes, for N_2 permeation.

Analyzing the behavior of the volumetric fluxes for every gas and PCL content, it can be seen that not every dense membrane appears below all asymmetric, meaning that some compositions do not represent any improvement despite their asymmetric character. Moreover, this results support what was stated when the thicknesses of dense layers were estimated and showed an improvement in gas permeation for PU5-1, PU5-5, PU15-1, PU15-5 and PU15-10, as shown below in this section.

A quick conclusion to take is asymmetric membranes with 5% and 10% PCL with 5 minutes of solvent evaporation time appear to be the best composition and have the optimal mode of preparation, along the fact that 5 wt.% was the most promising for medical devices requiring a short-term contact with blood and showed strong assets on the design of membranes with enhanced hemocompatibility, mainly with regard to platelet adhesion, as revealed in previous studies [5]. In addition, it is also known that states of fully spread platelet activation is inhibited for PCL contents of 5% [17].

Furthermore, unlike other compositions, the membrane that showed the best performance was the one with only 1 minute of solvent evaporation time. In addition, extreme states of platelet activation, spread and fully spread, are inhibited in membranes with 15 wt.% PCL [17].

To complete the comparation between the two types of membranes, assuming that the morphology of the dense layer of an asymmetric membrane is equal to a totally dense, which means that the characteristics remain the same, the thicknesses of the dense layers could be estimated using the permeabilities of nonporous Poly(ester urethane urea) (table 10) but applying the permeance values obtained for the asymmetric:

$$\delta = \frac{P}{perm \times 10^{10}} \tag{5}$$

Thereby, estimated values for dense layer's thickness are reported in table 10.

Table 10: Average estimated thicknesses and respective standard deviations for integral asymmetric membranes.

Membrane	Estimated Thickness, δ (mm)
PU5-1	0.109±0.004
PU5-5	0.104±0.005
PU5-10	0.122±0.003
PU10-1	0.132±0.021
PU10-5	0.122±0.016
PU10-10	0.145±0.024
PU15-1	0.089±0.005
PU15-5	0.097±0.008
PU15-10	0.109±0.007

The determination of this estimated values enabled the comparison with the ones in table 3 - total membrane thickness (figure 22).

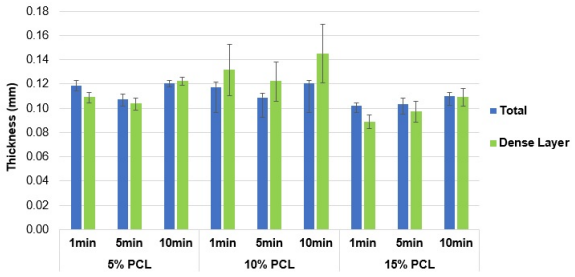

Figure 22: Comparison of total membrane thicknesses measured and estimated thickness values for integral asymmetric membranes.

Despite the results obtained for 10% PCL membranes where all the estimated thicknesses were higher than total membrane measured by hand which is not physically acceptable, for the other 2 compositions it was possible to observe a decrease of the variable under study (δ). Therefore, can be affirmed that, in this conditions, preparing an integral asymmetric instead of a totally dense membrane allowed a reduction of 8%, 3%, 13%, 6% and 1% of the dense layer for PU5-1, PU5-5, PU15-1, PU15-5 and PU15-10, respectively.

In fact, the permeance values obtained for the nonporous symmetric membranes present the same order of magnitude as the asymmetric membranes. These results may be due to the fact that membranes so-called asymmetrical are not entirely asymmetrical. This means that the pores observed on the bottom surface may not be interconnected so the gas molecules will have to diffuse from pore to pore through the membranes' core, acting like a dense membrane. Again, the problem may lie in the preparation of said membranes, more specifically, in the types of prepolymers used, the proportions between polymers and solvents or solvents among themselves and the solvent evaporation times, which maybe can be lowered.

4. Conclusions

Experimental tests were performed in a setup designed and optimized to allow high degrees of reproducibility and low uncertainty. This system aims to obtain more precise gas permeation measurements of membranes at a constant temperature and volume, by varying the feed pressure and monitoring the pressure difference evolution over time. Measurements were taken for three distinct gases, namely nitrogen, oxygen and carbon dioxide, with inlet pressures between 1 bar and 5 bar and using volumes of 13.5 cm^3 for the first two gases and 193.3 cm^3 for the last due to the sensibility of the equipment.

Nonporous PEUU were prepared using the solvent evaporation method with a solvent ratio (DMF/DEE) of 3/1 wt.% and polymer/solvent weight ratio of 65/35. Regarding the polymer compositions used, 4 different amounts of PCL were studied being 0, 5, 10 and 15 wt% corresponding to a 100, 95, 90 and 85 wt% content of PU (PU0, PU5, PU10 and PU15, respectively). SEM revealed completely dense surfaces (top and bottom), as well as the cross sections. When ready to use, said membranes were transparent, very sticky and slightly elastic, with average thicknesses of 0.112±0.006 mm, 0.115±0.004 mm, 0.107±0.004 mm and 0.112±0.001 mm, respectively.

Regarding the properties determined for nonporous PEUU, permeability, diffusion and solubility coefficients were calculated. The O_2 permeabilities assumed values equal to 22.9±0.4 Barrer, 20.1±0.3 Barrer, 18.2±0.4 Barrer and 16.5±0.5 Barrer while diffusion coefficients were $2.14 \pm 0.44 \times 10^{-6} cm^2/s$, $1.91 \pm 0.16 \times 10^{-6} cm^2/s$, $1.59 \pm 0.20 \times 10^{-6} cm^2/s$ and $1.74 \pm 0.12 \times 10^{-6} cm^2/s$ and solubility coefficients $(11.13 \pm 1.68) \times 10^{-4} cm^3/cm^3 cmHg$, $(10.64 \pm 0.93) \times 10^{-4} cm^3/cm^3 cmHg$, $(11.86 \pm 2.14) \times 10^{-4} cm^3/cm^3 cmHg$ and $(9.62 \pm 1.21) \times 10^{-4} cm^3/cm^3 cmHg$, for PU0, PU5, PU10 and PU15, respectively.

Concerning CO_2 and the variables determined, values equal to 230±0 Barrer, 198.3±1.3 Barrer, 218.0±36.1 Barrer and 168.1±0.5 Barrer for permeabilities while diffusion coefficients were $1.66 \pm 0.15 \times 10^{-6} cm^2/s$, $1.63 \pm 0.15 \times 10^{-6} cm^2/s$, $1.36 \pm 0.08 \times 10^{-6} cm^2/s$ and $1.42 \pm 0.08 \times 10^{-6} cm^2/s$ and solubility coefficients $(140.01 \pm 11.80) \times 10^{-4} cm^3/cm^3 cmHg$, $(123.25 \pm 12.92) \times 10^{-4} cm^3/cm^3 cmHg$, $(160.03 \pm 8.50) \times 10^{-4} cm^3/cm^3 cmHg$ and $(119.22 \pm 7.38) \times 10^{-4} cm^3/cm^3 cmHg$, for PU0, PU5, PU10 and PU15, respectively.

Finally, the results for N_2 were 9.9 Barrer, 7.4 Barrer, 10.1 Barrer and 6.7 Barrer for permeabilities while diffusion coefficients were $1.40 \pm 0.05 \times 10^{-6} cm^2/s$, $1.22 \pm 0.11 \times 10^{-6} cm^2/s$, $1.22 \pm 0.14 \times 10^{-6} cm^2/s$ and $1.00 \pm 0.02 \times 10^{-6} cm^2/s$ and solubility coefficients $(7.07 \pm 0.24) \times 10^{-4} cm^3/cm^3 cmHg$, $(6.14 \pm 0.60) \times 10^{-4} cm^3/cm^3 cmHg$, $(8.40 \pm 1.00) \times 10^{-4} cm^3/cm^3 cmHg$ and $(6.74 \pm 0.16) \times 10^{-4} cm^3/cm^3 cmHg$ in the same order of membranes.

Overall, it was possible to conclude that the highest fluxes are registered for CO_2, followed by O_2 and N_2, and higher permeabilities mostly result in higher solubility coefficients. Moreover, apart from the successive decrease in permeabilities for O_2 with the increase in PCL content, it was not possible to find a trend relating permeabilities, diffusion and solubility coefficients with the increase of said polymer, in the conditions described. Also, knowing the capacity of performance of the ideal oxygenator and considering a constant feed pressure of 2 bar, the membrane surface areas estimated varied between 13.5-17.5 m^2 for O_2 and 1.2-1.7 m^2 for CO_2, which means the first gas is the limiting factor in membrane development when it comes to the active surface areas. On the other hand, better hemocompatibility of the present membranes can make up the verified deficit on the O_2 side.

Further on, integral asymmetric PEUU were synthesized applying a modified phase inversion method, maintaining DMF/DEE proportions as well as the polymer/solvent ratio used for nonporous membranes, except the 0% PCL one. The times studied in the solvent evaporation phase, before consequent immersion in water, were 1, 5 and 10 minutes and measured thicknesses varied between 0.102 mm and 0.121 mm.

SEM showed that for the same solvent evaporation time, the amount of pores presented on the top surfaces decreases with the increase in PCL concentration, except for the 10 minutes case. Regarding the bottom surfaces, the exact opposite occurred since with the increase in PCL content there was an increase in pore density, as well as in pore diameter for evaporation times of 5 and 10 minutes. Finally, cross sections enabled the perception that for a polymer amount equal to 10% means a higher porosity and larger pores when compared to other compositions. SEM also revealed a decrease in pore density on the top surfaces with the increase of the time, except for membranes with compositions equal to 15% PCL. In all membranes was possible to observe a thin superficial layer that appears to be totally or almost totally dense. Contrary to what has been observed for symmetrical membranes, when ready for testing, porous membranes had a whitish and opaque appearance, were more elastic and easier to operate.

After comparing the effects of the different evaporation times applied and the 3 compositions studied it was concluded that,

apart from the fact that the largest fluxes continue to be observed for carbon dioxide, the permeance values, did not present great disparities with the variation of these variables. Also, no direct relationship was found between solvent evaporation time or wt% of PCL used with permeances.

Estimates made on the thickness of the dense layer revealed that the synthesis of asymmetrical membranes allowed a reduction of 8%, 3%, 13%, 6% and 1% for PU5-1, PU5-5, PU15-1, PU15-5 and PU15-10, in contrast to fully dense membranes. This result supported the improvement verified in gas permeation.

However, besides reviewing the preparation steps, the possible problems of reproducibility in the preparation of asymmetrical membranes, as well as the synthesis of thinner membranes with satisfactory resistance, could be solved by introducing the manufacture of supported membranes.

Finally, from the comparison of both types of membrane including all three different compositions and the diverse evaporation times, it was possible to realize that the best compositions and, consequently, preparation methods were 5% PCL with 5 minutes of solvent evaporation time and 15% PCL with 1 minute.

5. Perspectives for Future Work

Next step would consist in testing all the same membranes reported in the present work in a gas-liquid system to make sure the behaviour observed is consistent, since in a real ECMO the exchange is carried out through a membrane from blood to gas and vice versa.

Furthermore, having selected the membranes with the best performance, it would be of great interest to introduce microfibers on the surface of the active layer, for example, through an electrospining technique, in order to promote the mixing and disruption of the diffusive boundary layer and improve mass transfer.

Gas permeation of modified membranes must be tested in both existing gas/membrane/gas setup, as well as in the gas/membrane/liquid.

Plus, manufacturing supported membranes would be important to eliminate possible problems of reproducibility as well as improving the resistance of thinner membranes. Characterize and perform gas permeation tests in gas-gas and gas-liquid systems.

References

[1] "Membranes for the Life Sciences," in *Membrane Technology* (K.-V. Peinemann and S. Pereira Nunes, eds.), vol. 1, Wiley-VCH, 2007.

[2] N. C. Nanda, N. Trehan, B. Airan, S. A. Conrad, and Y. Mehta, *Manual of Extracorporeal Membrane Oxygenation (ECMO) in the ICU*. 2014.

[3] D. F. Stamatialis, B. J. Papenburg, M. Giron, S. N. M. Bettahalli, S. Schmitmeier, and M. Wessling, "Medical applications of membranes : Drug delivery , artificial organs and tissue engineering," vol. 308, pp. 1–34, 2008.

[4] H. Iwahashi, K. Yuri, and Y. Nosé, "Development of the oxygenator: Past, present, and future," *Journal of Artificial Organs*, vol. 7, no. 3, pp. 111–120, 2004.

[5] M. C. Besteiro, A. J. Guiomar, C. A. Gonçalves, V. A. Bairos, M. N. De Pinho, and M. H. Gil, "Characterization and in vitro hemocompatibility of bi-soft segment, polycaprolactone-based poly(ester urethane urea) membranes," *Journal of Biomedical Materials Research - Part A*, vol. 93, no. 3, pp. 954–964, 2010.

[6] M. Faria, V. Geraldes, and M. N. De Pinho, "Surface characterization of asymmetric Bi-soft segment poly(ester urethane urea) membranes for blood-oxygenation medical devices," *International Journal of Biomaterials*, vol. 2012, 2012.

[7] M. Faria and M. N. de Pinho, "Phase segregation and gas permeation properties of poly(urethane urea) bi-soft segment membranes," *European Polymer Journal*, vol. 82, pp. 260–276, 2016.

[8] M. Faria, M. Rajagopalan, and M. N. De Pinho, "Tailoring bi-soft segment poly (ester urethane urea) integral asymmetric membranes for CO2 and O2 permeation," *Journal of Membrane Science*, vol. 387-388, no. 1, pp. 66–75, 2012.

[9] T. M. Eusébio, "Polyurethane urea membranes for membrane blood oxygenators : synthesis and gas permeation properties," *Instituto Superior Técnico MSc Thesis*, November 2017.

[10] G. Pon, "Gas permeation in bi-soft segment poly (ester urethane urea) membranes for Membrane Blood Oxygenators," *Instituto Superior Técnico MSc Thesis*, November 2018.

[11] F. Wiese, "Membranes for Artificial Lung and Gas Exchange Applications," in *Biomedical Membranes and (Bio)Artificial Organs* (D. Stamatialis, ed.), vol. 2, ch. 4, pp. 83–104, 2018.

[12] D. N. Gray, "Polymeric Membranes for Artificial Lungs.," in *Polymeric Materials and Artificial Organs* (C. G. Gebelein, ed.), ch. 9, pp. 151–162, 1984.

[13] R. W. Baker and B. T. Low, "Gas separation membrane materials: A perspective," *Macromolecules*, vol. 47, no. 20, pp. 6999–7013, 2014.

[14] S. W. Rutherford and D. D. Do, "Review of time lag permeation technique as a method for characterisation of porous media and membranes," *Adsorption*, vol. 3, no. 4, pp. 283–312, 1997.

[15] R. Perry, D. Green, and J. Maloney, *Chemical Engineer Handbook*. McGraw-Hill, 7 ed., 1997.

[16] M. Mulder, *Basic Principles of Membrane Technology*. Springer Netherlands, 2 ed., 1997.

[17] M. Faria, P. Brogueira, and M. N. de Pinho, "Sub-micron tailoring of bi-soft segment asymmetric polyurethane membrane surfaces with enhanced hemocompatibility properties," *Colloids and Surfaces B: Biointerfaces*, vol. 86, no. 1, pp. 21–27, 2011.